High-accuracy energy formulas for the attractive two-site Bose-Hubbard model

Igor Ermakov*
New York University Shanghai, 1555 Century Avenue, Pudong, Shanghai 200122, China
and ITMO University, Kronverkskiy 49, 197101, St. Petersburg, Russia

Tim Byrnes†
State Key Laboratory of Precision Spectroscopy, School of Physical and Material Sciences,
East China Normal University, Shanghai 200062, China;
New York University Shanghai, 1555 Century Avenue, Pudong, Shanghai 200122, China;
NYU-ECNU Institute of Physics at NYU Shanghai, 1555 Century Avenue, Pudong, Shanghai 200122, China;
National Institute of Informatics, 2-1-2 Hitotsubashi, Chiyoda-ku, Tokyo 101-8430, Japan;
and Department of Physics, New York University, New York, New York 10003, USA

Nikolay Bogoliubov
St. Petersburg Department, V.A. Steklov Mathematical Institute, Russian Academy of Sciences, Fontanka 27, St. Petersburg, 191023, Russia
and ITMO University, Kronverkskiy 49, 197101, St.Petersburg, Russia

(Received 29 August 2017; published 20 February 2018)

The attractive two-site Bose-Hubbard model is studied within the framework of the analytical solution obtained by the application of the quantum inverse scattering method. The structure of the ground and excited states is analyzed in terms of solutions of Bethe equations, and an approximate solution for the Bethe roots is given. This yields approximate formulas for the ground-state energy and for the first excited-state energy. The obtained formulas work with remarkable precision for a wide range of parameters of the model, and are confirmed numerically. An expansion of the Bethe state vectors into a Fock space is also provided for evaluation of expectation values, although this does not have accuracy similar to that of the energies.

DOI: 10.1103/PhysRevA.97.023626

I. INTRODUCTION

Interacting indistinguishable bosonic systems capture a wide variety of physical systems, from cold atoms [1], photons [2], and elementary excitations in solid state systems [3] such as excitons, magnons, polaritons, and phonons, to elementary particles such as gluons [4]. The ability to produce and control identical bosons has improved vastly over the last few decades. Bose-Einstein condensation [5,6] allows the preparation of interacting bosonic systems in traps of highly flexible geometry. For example, to produce large arrays of trapped bosons, cold atoms can be placed in optical lattices [7], and exciton polaritons can be etched or patterned [8] for the purposes of quantum simulation [9]. Although not strictly bosonic, superconductors also have exquisite engineering capability that realized a quantum phase transition to a Mott insulating phase early on [10]. The achievement of the Bose-Einstein condensation of photons [11] and magnons [12,13] may also make it possible for similar engineering to be performed in other systems.

One of the most simple and experimentally relevant configurations in this context is a system of a large number of interacting two-species bosons. This could be realized, for example, by a Bose-Einstein condensate (BEC) in a double-well trap [14] (Fig. 1), or bosons with two internal states [15]. Despite its simplicity, many interesting phenomena have been investigated in the past using this basic configuration, such as a single bosonic Josephson junction [16] and matter-wave interferometry [17]. By taking advantage of the natural interaction between the bosons, squeezing of quantum states can be performed for use in quantum metrology [18–20]. Many theoretical studies has also been carried out within this concept and beyond; for example, the Einstein-Podolsky-Rosen (EPR) paradox has been considered [21,22], as well as different quantum dynamics such as the revivals and decoherence [23–25]. Investigations toward using such system as the basis of quantum computing have also been performed [26,27].

Due to the wide applicability of the model, solutions for the ground- and excited-state energies and wave functions are of direct interest to compare to experiment. The problem mathematically can be described by two-site Bose-Hubbard model in the two-mode approximation [28]. One of the most common approaches to the model is a straightforward numerical investigation; see, for example, [22]. Some good approximations to the tunneling frequency have also been obtained by means of a Bohr-Sommerfeld quantization approach [29]. The model was solved exactly by the application of the quantum inverse scattering method (QIM) [30], see also Ref. [31] for a review. The QIM [32,33] allows us to define some special class of exactly solvable or integrable models. The property of

*ermakov1054@yandex.ru
†tim.byrnes@nyu.edu

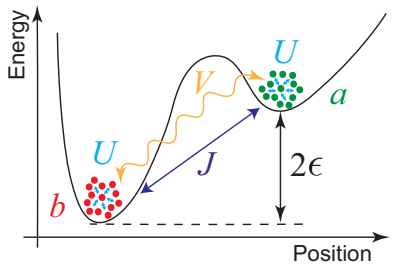

FIG. 1. Two-site Bose-Hubbard model realized by an asymmetric double-well trap. The energy difference between the two wells is 2ϵ, the tunneling occurs with amplitude J, the on-site interaction between the atoms in the same well is U, and the interwell interaction is V. We consider the attractive regime where $U < V$.

integrability allows one to obtain exact, nonperturbative results for eigenenergies and time-dependent correlation functions. Originally the QIM was mainly developed in Refs. [34–36]; for an extensive review, see Refs. [37–39]. The QIM is one of the most powerful tools for analyzing one-dimensional strongly correlated systems, for example, in spin chains [38,40–42] or for one-dimensional BECs [43,44]. Furthermore the QIM can be applied to problems in areas such as quantum optics [45], string theory [46], and random walks [47]. For the two-site Bose-Hubbard model, the determinant representation for time-dependent correlation functions has been developed [48], and the expansion of the eigenfunctions of the model into Fock space was been performed in Ref. [49].

Despite the fact that the mathematical solutions of the two-site Bose-Hubbard model are well developed, the cornerstone of practical implementation of QIM are the Bethe equations, which are a set of coupled nonlinear algebraic equations. The explicit form of Bethe equations depend crucially on the model under consideration. For some special cases it can be solved analytically [33], whereas for most cases it requires significant computational power. For other models several different techniques of solving Bethe equations have been developed [50–53]. For the two-site Bose-Hubbard model, no effective technique of solving Bethe equations has been developed so far. This has made the evaluation of the exact solutions using QIM rather cumbersome and has hindered their practical use as a tool to analyze the model.

In this paper, we analyze the structure of the Bethe equations for the attractive two-site Bose-Hubbard model. We describe the ground state and the elementary excitations of the model in terms of solutions of the Bethe equations. Approximate solutions of the Bethe equations are given, which in turn can be used to obtain approximate formulas for the ground-state energy and for the first excited-state energy. We find that due to the power of the QIM method, the approximate solutions give extremely precise expressions for the energy which can be evaluated relatively straightforwardly. These are numerically confirmed and we analyze the level of accuracy attained. These solutions can in principle be used to evaluate expectation values as well, although the accuracy is not as high as for energies.

The paper is organized as follows. In Sec. II we give an overview of the two-site Bose-Hubbard model, the traditional approach to the eigenvalue problem, and general properties of the spectrum. We introduce an auxiliary Hamiltonian which is more convenient from the standpoint of the QIM. In Sec. III we provide a short review of the results obtained by application of the QIM to the model under consideration. For our purposes we need only Bethe equations and the expression for spectrum of the model. In Sec. IV A we analyze the structure of elementary excitations of the model in terms of solutions of Bethe equations. We provide a numerical analysis of Bethe equations and also propose and motivate several statements about general structure of solutions of Bethe equations. In Sec. IV B we introduce the equidistant approximation for the solutions of Bethe equations and using it we obtain the approximate formulas for the ground state of the model. In Sec. IV C by applying the equidistant approximation we derive the approximated formulas for the first excited state of the model. We also discuss the behavior of solutions of Bethe equations under some certain transformations and find a singular point in the solution. In Sec. V we discuss the application of the equidistant approximation to the evaluation of expectation values. Finally, in Sec. VI we summarize and discuss the primary results of the paper.

II. TWO-SITE BOSE-HUBBARD MODEL

The system considered in this paper is the two-site Bose-Hubbard model, which is described by the Hamiltonian

$$\hat{\mathcal{H}} = \epsilon(a^\dagger a - b^\dagger b) - J(a^\dagger b + a b^\dagger) + \frac{U}{2}(a^\dagger a^\dagger a a + b^\dagger b^\dagger b b) + V a^\dagger a b^\dagger b, \tag{1}$$

where $a, a^\dagger$ and $b, b^\dagger$ are bosonic creation and annihilation operators, respectively, in each site satisfying $[a, a^\dagger] = [b, b^\dagger] = 1$, and operators on different sites commute. The total number operator of particles $\hat{N} = a^\dagger a + b^\dagger b$ is conserved: $[\hat{\mathcal{H}}, \hat{N}] = 0$. Here, ϵ is the bias potential, J is the tunneling between the wells, U is the on-site interaction energy, and V is the intersite interaction energy. We define $U - V > 0$ to be a repulsive regime, where the interaction energy is minimized by distributing the atoms evenly between the wells. Conversely, for $U - V < 0$ the atoms are in an attractive regime, where the interaction energy is minimized by having all atoms in the same well.

The above model can be realized in various different ways. In Fig. 1 we show one possible realization of the two-site Bose-Hubbard model, where N bosons are placed in an asymmetric double-well trap, and the two-mode approximation is made [28]. The symmetric double-well trap corresponds to setting $\epsilon = 0$. For cold neutral atoms in mean-field approximation, the interaction can be expressed $U = \frac{4\pi\hbar^2 a}{m}$, where a is the s-wave scattering length [54], and can be tuned using Feshbach resonances [55]. For the intersite interaction energy V, this may arise from a long-range interaction in the BEC, for example, by a spin-orbit-coupling [56] or dipole-dipole interaction [57]. The bias ϵ may be positive or negative, depending on the energy detuning between the two modes. Another way that the two-site Bose-Hubbard model could be realized is where the two modes are defined by two hyperfine spin states. In this case U and V are determined by the interactions between the same and different spin species. Similar Hamiltonians have been examined to study miscible-immiscible transitions controlled by the ratio of

U and V [58]. For the details of the experimental realization of the Hamiltonian (1), the reader can see, for example, Ref. [14]. Typical range for parameters ϵ, J, U, and V can be found, for example, in Refs. [5,56].

Consider the eigenvalue problem for the above Hamiltonian

$$\hat{\mathcal{H}}\left|\Psi_N^\sigma\right\rangle = \mathcal{E}_N^\sigma\left|\Psi_N^\sigma\right\rangle, \tag{2}$$

where σ labels the eigenstates $\sigma = 0,\ldots,N$. Since the Hamiltonian conserves total particle number N, the wave function can be expanded as

$$\left|\Psi_N^\sigma\right\rangle = \sum_{n=0}^{N} \mathcal{A}_n^{N,\sigma}|N-n\rangle_a|n\rangle_b, \tag{3}$$

where $|m\rangle_q = (m!)^{-1/2}(q^\dagger)^m|0\rangle_q$, $(q = a,b)$ are the number of particles in a and b traps, respectively. The states (3) form a complete orthogonal set. Amplitudes $\mathcal{A}_n^{N,\sigma}$ satisfy the matrix equation

$$\begin{aligned}\mathcal{E}_N^\sigma \mathcal{A}_n^{N,\sigma} &= \left[\epsilon(N-2n) + (U-V)n(n-N) + \frac{U}{2}N(N-1)\right]\mathcal{A}_n^{N,\sigma} \\ &\quad - J\sqrt{(n+1)(N-n)}\mathcal{A}_{n+1}^{N,\sigma} - J\sqrt{n(N-n+1)}\mathcal{A}_{n-1}^{N,\sigma},\end{aligned} \tag{4}$$

where the rank of this equation is $N+1$. The spectrum $\mathcal{E}_N^\sigma(\epsilon,J,U,V)$ of Hamiltonian (1) possesses the following properties:

$$\begin{aligned}&\mathcal{E}_N^\sigma(\epsilon,J,U,V) = \mathcal{E}_N^\sigma(-\epsilon,J,U,V) = \mathcal{E}_N^\sigma(\epsilon,-J,U,V), \\ &\mathcal{E}_N^\sigma(\epsilon,J,U,V) = -\mathcal{E}_N^{N-\sigma}(\epsilon,J,-U,-V).\end{aligned} \tag{5}$$

In the limit of zero interaction $U = V = 0$, one can simply diagonalize Hamiltonian (1) by a linear transformation of the boson operators to obtain the spectrum

$$\mathcal{E}_N^\sigma(\epsilon,J,0,0) = \sqrt{\epsilon^2+J^2}(2\sigma - N). \tag{6}$$

For the application of the QIM it is convenient to introduce another Hamiltonian. The conservation of the total number operator allows us to define an equivalent Hamiltonian with an energy offset and rescaling [48]:

$$\hat{H} = -\frac{1}{J}\left(\hat{\mathcal{H}} - \frac{U}{2}\hat{N}(\hat{N}-1) - \epsilon\hat{N}\right), \tag{7}$$

which satisfies $[\hat{H},\hat{\mathcal{H}}] = 0$. This can be explicitly written as

$$\hat{H} = a^\dagger b + ab^\dagger + \Delta b^\dagger b + c^2 a^\dagger a b^\dagger b, \tag{8}$$

where

$$c^2 = \frac{U-V}{J}, \quad \Delta = \frac{2\epsilon}{J} \tag{9}$$

are the rescaled interaction strength and detuning, respectively. The introduced parameters c^2 and Δ are dimensionless, so the eigenenergies of Hamiltonian (8) are dimensionless as well. Henceforth we can consider $\hat{H}$ and give its exact solution, but the same results can immediately be extended to the model with Hamiltonian (1) through the mapping given above.

The eigenvalue problem for Hamiltonian (8),

$$\hat{H}\left|\Psi_N^\sigma\right\rangle = E_N^\sigma\left|\Psi_N^\sigma\right\rangle, \tag{10}$$

can equally be solved by applying the expansion (3) for $|\Psi_N^\sigma\rangle$. Denoting the amplitudes of the expansion in this parametrization by $A_n^{N,\sigma}$, the matrix equation is

$$\begin{aligned}E_N^\sigma A_n^{N,\sigma} &= [\Delta n + c^2 n(N-n)]A_n^{N,\sigma} + \sqrt{n(N-n+1)}A_{n-1}^{N,\sigma} \\ &\quad + \sqrt{(n+1)(N-n)}A_{n+1}^{N,\sigma}.\end{aligned} \tag{11}$$

From the energy eigenvalue E_N^σ of Hamiltonian (8), we can find the energy $\mathcal{E}_N^\sigma$ of Hamiltonian (1) using the mapping (7)

$$\mathcal{E}_N^\sigma = -JE_N^\sigma + \frac{U}{2}N(N-1) + \epsilon N. \tag{12}$$

In this paper we consider only the attractive case $U - V < 0$. For simplicity we suppose that ϵ and J are always negative, so the constants c^2 and Δ are always positive. From the symmetries in Eq. (5), this can be assumed without loss of generality. From the relation (5) we observe that the ground state of the attractive case is the highest energy excitation for the repulsive case and vice versa. Hence, our results for the attractive case can be mapped to the repulsive case in this sense. However, since we assume that the ground and low energy states are most important in practice, our results will be mostly relevant to the attractive case. We note that for attractive BECs there is typically a limit to the maximum number of atoms due to the development of vibrational instabilities [59]. Although an unconfined attractive BEC is always unstable, this can be overcome by setting a suitably tight confining trap. In this sense, for a particular physical implementation, there may be inaccessible parameter ranges. In writing Eq. (1) we have assumed that the system is suitably prepared such that the BEC is stable.

III. QUANTUM INVERSE METHOD

The model described by Hamiltonian (1) is exactly solvable. It was first solved by the application of the QIM in Ref. [30]. The QIM allows the construction of a complete orthogonal set of eigenfunctions and finds its corresponding energy spectrum. In this context it is more convenient to consider Hamiltonian (8), in terms of the parameters c and Δ. In this section we summarize the main results of the solution obtained by the QIM; for a detailed explanation of the application of the QIM to Hamiltonian (8) see Ref. [48].

The energy spectrum E_N^σ of Hamiltonian (8) is given by [48]

$$E_N^\sigma = -\frac{1}{c^2} + \frac{1}{c^2}\prod_{j=1}^{N}\left(1 + \frac{c}{\lambda_j^\sigma}\right), \tag{13}$$

where the roots λ_j^σ are defined as the solutions of N Bethe equations

$$c\lambda_n^\sigma\left(c\lambda_n^\sigma + \Delta\right) = \prod_{j=1,j\neq n}^{N}\frac{\lambda_n^\sigma - \lambda_j^\sigma - c}{\lambda_n^\sigma - \lambda_j^\sigma + c}. \tag{14}$$

We denote the solution of the Bethe equations (14) as $\Lambda_N^\sigma = \{\lambda_1^\sigma,\lambda_2^\sigma,\ldots,\lambda_N^\sigma\}$, where $\sigma = 0,1,\ldots,N$ is a label for the energy levels of the system. The QIM demands that all roots λ_i^σ in one solution be different $\forall\ \lambda_{i,j}^\sigma \in \Lambda_N^\sigma \Rightarrow \lambda_i^\sigma \neq \lambda_j^\sigma$, such that the solution describes a physical state [33]. There are $N+1$ solutions Λ_N^σ which satisfy this condition, and each of them corresponds to a certain energy level E_N^σ.

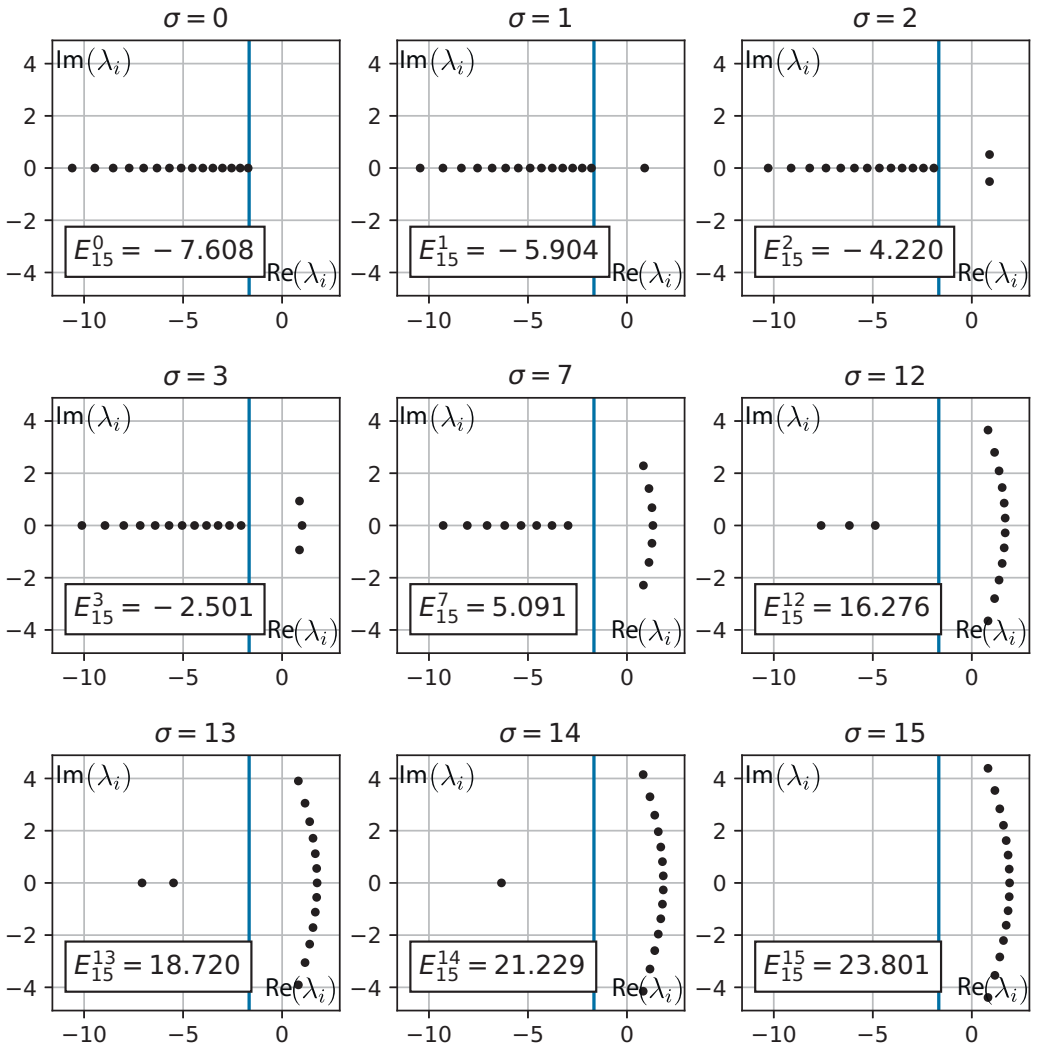

FIG. 2. Solutions Λ^{σ}_{15} of the Bethe equations (14) on the complex plane. The parameters are $c = 0.3$, $\Delta = 0.5$, and $N = 15$. The vertical solid line is equal to $-\frac{\Delta}{c}$.

The complex conjugation of each root $(\lambda^{\sigma}_i)^*$ belongs to the same solution $\forall\, \lambda^{\sigma}_i \in \Lambda^{\sigma}_N \;\Rightarrow (\lambda^{\sigma}_i)^* \in \Lambda^{\sigma}_N$ [60]. This ensures that the energy in Eq. (13) is always real. It is evident that if N is even we have an even number of purely real roots in the solution Λ^{σ}_N whereas if N is odd we have an odd number of purely real roots. A typical root distribution is depicted in Fig. 2; a more detailed explanation of this picture will be provided in the next section. It is also straightforward to verify that Eq. (14) possesses the following symmetry: shifting the solution of the Bethe equations for parameters (c, Δ) by $\lambda^{\sigma}_n \to \lambda^{\sigma}_n - \Delta/c$ results in another solution for the parameters $(c, -\Delta)$. It is also straightforward to check that there are no other constant shifts which can generate more solutions.

In general, the set of solutions $\{\Lambda^{\sigma}_N\}^N_{\sigma=0}$ of the Bethe equations (14) contains complete information not only about eigenenergies of Hamiltonian (8) but about its eigenfunctions as well. Therefore, any observable can be expressed in terms of the roots. Eigenfunctions being expressed via roots are usually called Bethe vectors. In Ref. [30] such Bethe vectors were constructed for the two-site Bose-Hubbard model. Reference [48] gives the Bethe vectors for Hamiltonian (8).

IV. APPROXIMATE SOLUTIONS OF THE BETHE EQUATIONS

To extract physical observables from the QIM, one is faced with the task of solving the Bethe equations. Equations (14) are a set of N coupled algebraic nonlinear equations. Solving the system of equations (14), even numerically, is a nontrivial task for realistic systems where the total number of particles N is large. Considering that the original matrix equations (11) are also an eigenvalue problem in $N + 1$ equations, it may appear that solving the original set of equations is a simpler and more straightforward approach. However, we show here that it is not always necessary to know the exact solution Λ^{σ}_N of the Bethe equations to extract information about observables. In this section we demonstrate how we can obtain some information about energy levels of the system without solving the Bethe equations explicitly.

A. Structure of the Bethe solutions

To start, let us first make a guess of a suitable distribution of roots $\Lambda^0_N = \{\lambda^0_1, \lambda^0_2, \ldots, \lambda^0_N\}$, which can potentially satisfy the

Bethe equations (14), and which can also minimize the energy (13). To minimize energy E_N^0 let us suppose that for the ground state, all the roots λ_i^0 are real and negative. Using the data obtained from various numerical solutions of Bethe equations we can make another assumption that $c\lambda_1^0(c\lambda_1^0+\Delta)\to 0$, so λ_1^0 can be either close to zero $\lambda_1^0\to 0$ or be equal to $\lambda_1^0=-\frac{\Delta}{c}$. For $\lambda_1^0\to 0$ the energy E_N^0 will be increased significantly and may be positive, so we suppose that $\lambda_1^0=-\frac{\Delta}{c}$. This assumption can also be justified by the fact that for large c the ground-state energy goes to zero; it will become clear below that this would be impossible without this assumption. The right-hand side of the first Bethe equation should then be zero:

$$\prod_{j=2}^{N}\frac{\lambda_1^0-\lambda_j^0-c}{\lambda_1^0-\lambda_j^0+c}=0. \tag{15}$$

One obvious way to satisfy Eq. (15) is to pick $\lambda_2^0=-\frac{\Delta}{c}-c$. Now if we demand the remaining λ_i^0 to be less than λ_2^0, the energy E_N^0 will always be negative. To minimize E_N^0, the remaining λ_i^0 should be as small as possible and negative, while still satisfying the Bethe equations. The Bethe equations (14) require all the roots λ_i to be separated by some finite range. The least possible range between two different roots is equal to c. Indeed, if we have $\Lambda_N^0:\forall\,\lambda_i^0\neq\lambda_j^0\in\Lambda_N^0\Rightarrow|\lambda_i^0-\lambda_j^0|>c$, the right side of the Bethe equations will always be positive, as it should be, because $\forall\,\lambda_n^0\Rightarrow c\lambda_n^0(c\lambda_n^0+\Delta)>0$.

The exact numerical solution of the Bethe equations for typical parameters and a relatively small particle number $N=15$ is shown in Fig. 2. Although the numerical values of the solutions depend on the particular parameters chosen, from Fig. 2, where $\sigma=0$, it can be seen that the basic structure for ground state is always the same. That is, the roots always have zero imaginary parts and are negative, they are also always separated from zero by a gap whose value is $-\frac{\Delta}{c}$, and the distance between two different roots is always bigger than c.

An M-hole type excitation can be generated by removing M particles from the N-particle ground state, as shown in Fig. 2. Such a picture is analogous to the ground state of fermions, where we create an excitation by removing the particle under the Fermi sphere. In the QIM, however, the roots themselves do not directly relate to a physical observable, although in some cases the root can be associated with the quasimomentum of the particle, for example, in the Lieb-Liniger model [43].

B. Ground state

1. Approximate energy formula

From the general expression for the energy in Eq. (13), it is easy to see that large values of λ_n^σ only give a small correction to the energy. In view of this, it is more important to obtain a good estimate for the small values of λ_n^σ. Using the assumptions made above about distribution of the roots for the ground state, we propose the following equidistant approximation:

$$\lambda_n^0\approx-\frac{\Delta}{c}-c(n-1), \tag{16}$$

where $n=1,\ldots,N$. This formula predicts a first few roots extremely well and the level of approximation becomes worse as n increases. Notice that despite the fact that Eq. (16) predicts several first roots with great precision, the approximated roots can never exactly coincide with the roots from actual solutions. The direct substitution of Eq. (16) into Eq. (14) will eventually lead to the contradiction. Actual solutions of the Bethe equations (14) are always slightly different from those ones predicted by Eq. (16), the numerical discrepancy can be negligible but it always exists. Substituting Eq. (16) into Eq. (13) we obtain an approximate expression for the ground-state energy:

$$E_N^0\approx-\frac{N+1}{c^2(N-1)+\Delta}. \tag{17}$$

Using the formulas (12) and (17) we can find the ground-state approximation for Hamiltonian (1)

$$\mathcal{E}_N^0\approx\frac{J^2(N+1)}{(U-V)(N-1)+2\epsilon}+\frac{U}{2}N(N-1)+\epsilon N. \tag{18}$$

2. Error analysis

In Figs. 3–5 we plot the relative error

$$\xi(X)=\left|\frac{X_{\text{approx}}-X_{\text{exact}}}{X_{\text{exact}}}\right|, \tag{19}$$

where X_{exact} and X_{approx} are the exact and approximate values. In Figs. 3 and 4 we analyze the relative error of Eqs. (17) and (18) compared to numerically obtained values using exact diagonalization. Formula (17) works with high precision for a wide range of parameters except for small dimensionless interactions $c^2<0.01$ for the particle numbers in the range $N>100$. The fact that the approximation breaks down for

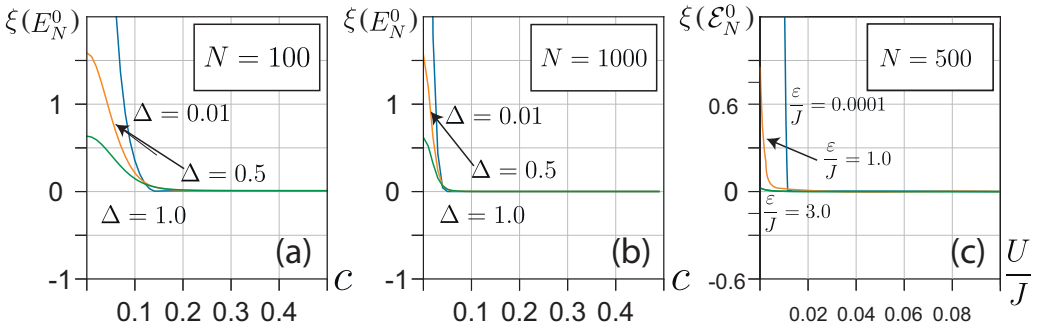

FIG. 3. Relative error for the approximated formula (17) vs c for different values of $\Delta=0.01,0.5,1$, for (a) $N=100$ and (b) $N=1000$. (c) Relative error for the approximated formula (18) vs U/J for marked values of ε/J, and for $V=0$ and $N=100$.

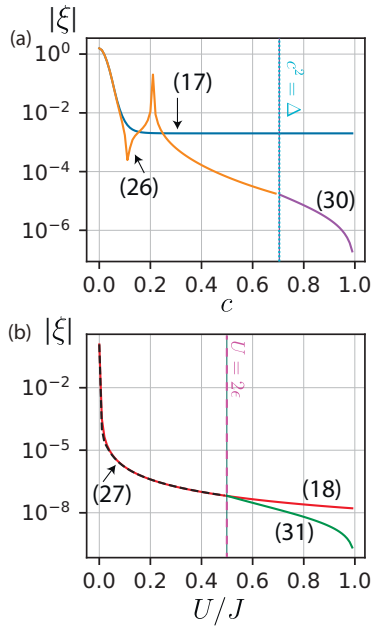

FIG. 4. The relative error ξ for all the approximate formulas in this paper versus the dimensionless interaction c. The chosen physical parameters are $\varepsilon/J = 0.25, V = 0, N = 500$, which correspond to $\Delta = 0.5$ in (8). The dashed vertical line corresponds to the special point $U = 2\epsilon$, whereas the dotted one corresponds to the value of $c = \sqrt{\Delta} = \sqrt{0.5}$.

small c is not surprising because the point $c = 0$ is singular for the Bethe equations (14). The Bethe solution has the property that it works better when the interactions are strong. In this way it is complementary to perturbative techniques expanding around the limit of zero interaction. It can be seen from Fig. 3 that Eq. (17) improves in accuracy as N is increased, and has a fairly small dependence on Δ. Since the range $c^2 = (U - V)/J < 0.01$ corresponds to physically a rather small value, the results suggest that our formulas give a powerful way of evaluating the energies. In Fig. 5 the dependence of the relative error of the formulas on N is shown for typical values. The straight line on the log-log plot suggests a effective power-law dependence of the error

$$\xi \sim N^{-\alpha}. \tag{20}$$

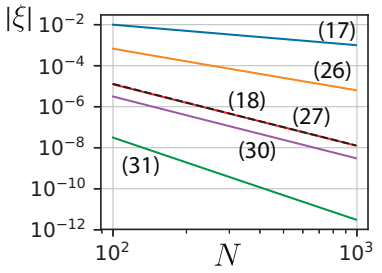

FIG. 5. Relative error ξ for all the approximation formulas of the paper, for different $N \in [100, 1000]$. Here the parameters are $\epsilon = -0.25$, $J = -1.0$, $U = -0.4$, and $V = 0.0$, and correspondingly $\Delta = 0.5$ and $c = \sqrt{0.4}$; and for Eqs. (27) and (28), $c = -U = 1.0$.

We estimate from Fig. 5 that Eq. (17) has a scaling as $\alpha \simeq 1.0$, and Eq. (18) $\alpha \simeq 2.9$.

C. First excited state

The procedure described above can be applied to finding the energy of the first excited state. We consider two parameter ranges $c^2 < \Delta$ and $c^2 > \Delta$ which must be handled differently due to reasons we explain below.

1. Approximate energy formula for $c^2 < \Delta$

According to Sec. IV A, the first excited state $\lambda \in \Lambda_N^1$ can be found by removing the smallest root λ_N^0 from the ground state Λ_N^0, and moving it to a positive value $\lambda_1^1 \equiv \lambda > 0$, yet to be determined. The remaining roots are left unchanged with respect to the ground state such that

$$\lambda_n^1 = -\frac{\Delta}{c} - c(n-2), \tag{21}$$

for $n = 2, \ldots, N$. From the first equation of Eq. (14), λ should satisfy

$$c\lambda(c\lambda + \Delta) = \prod_{j=2, j\neq n}^{N} \frac{\lambda - \lambda_j^1 - c}{\lambda - \lambda_j^1 + c}. \tag{22}$$

Substituting Eq. (21) into Eq. (22) we obtain

$$\prod_{j=2, j\neq n}^{N} \frac{\lambda - \lambda_j^1 - c}{\lambda - \lambda_j^1 + c} = \frac{\left(\lambda + \frac{\Delta}{c} - c\right)\left(\lambda + \frac{\Delta}{c}\right)}{\left[\lambda + \frac{\Delta}{c} + c(N-2)\right]\left[\lambda + \frac{\Delta}{c} + c(N-1)\right]}. \tag{23}$$

Simplifying this expression we obtain

$$c^2\lambda = \frac{\lambda + \frac{\Delta}{c} - c}{\left[\lambda + \frac{\Delta}{c} + c(N-2)\right]\left[\lambda + \frac{\Delta}{c} + c(N-1)\right]}, \tag{24}$$

which has three solutions. Assuming that λ is positive and small, we discard terms which are proportional to λ^2 and λ^3, yielding

$$\lambda = \frac{\Delta - c^2}{[c^2(N-2) + \Delta][c^2(N-1) + \Delta]c - c}. \tag{25}$$

We assume that N is large so the denominator of Eq. (24) is always positive, whereas the numerator becomes negative when $c^2 > \Delta$. This fact places us a restriction on our approximation, because λ should be positive. Nevertheless, the approximate formula for the first excited state still can be found for the case $c^2 > \Delta$, which we discuss in the next section. Substituting Eqs. (21) and (25) into Eq. (13) we obtain the following approximate formula for the first excited-state energy:

$$E_N^1 \approx c^2(N-1) - \frac{N}{c^2(N-2) + \Delta} + \Delta, \tag{26}$$

which is valid for $c^2 < \Delta$. In terms of the physical variables, using Eqs. (12) and (26) we can equally write this as

$$\mathcal{E}_N^1 \approx \epsilon(N-2) - (U-V)(N-1) + \frac{U}{2}N(N-1) + \frac{J^2 N}{(U-V)(N-2) + 2\epsilon}, \tag{27}$$

which is valid for $U - V < 2\epsilon$.

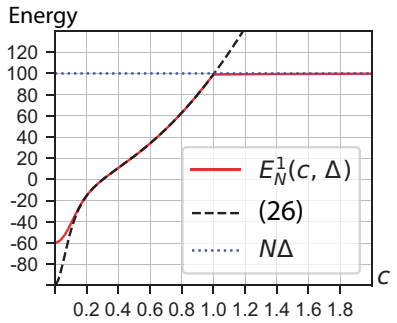

FIG. 6. First excited-state energy vs c. Parameters used are $\Delta = 1.0$ and $N = 100$. Solid line shows the exact solution, dashed line is the approximated energy of Eq. (26), horizontal dotted line is $N\Delta$.

2. *Approximate energy formula for $c^2 > \Delta$*

Due to the restrictions described above, Eqs. (26) and (27) are not valid for $c^2 > \Delta$. In Fig. 6 we compare the exact and approximate energies as derived above. Evidently the behavior of the first excited-state energy E_N^1 dramatically changes at the point $c^2 = \Delta$. To understand the origin of this, let us examine the Hamiltonian

$$\hat{H}_Z = \Delta b^\dagger b + c^2 a^\dagger a b^\dagger b, \tag{28}$$

which corresponds to Eq. (8) with the tunneling terms turned off. Since the above Hamiltonian does not possess any off-diagonal terms, the eigenstates of Eq. (28) are simply number states $|n, N-n\rangle$ with energy

$$E_{ZN}^n = (N-n)(\Delta + c^2 n), \tag{29}$$

where $n = 0, \ldots, N$. For attractive interactions $U - V < 0$ and a large number of particles, the energy is minimized by having all the bosons in the same mode a or b. Thus there are two states $|N,0\rangle$ and $|0,N\rangle$ which are split by the presence of the bias field Δ. The spectrum of Hamiltonian (28) is presented in Fig. 8. As can be seen, if $c^2 > \Delta$ the first excited state is the state $|0,N\rangle$, whereas if $c^2 < \Delta$ the state is $|N-1,1\rangle$. Thus the nature of the first excited state changes dramatically depending upon what regime the parameters are in.

This phenomenon can also be seen by analyzing the solutions $\Lambda_N^1(c,\Delta)$ of Bethe equations (14). Solving Eqs. (14) numerically, we find that under the transformation $c \to c'$, the solutions smoothly transition from $\Lambda_N^1(c,\Delta) \to \Lambda_N^1(c',\Delta)$ as long as c does not cross the point $c^2 = \Delta$. Once c crosses this point, the solution $\Lambda_N^1(c,\Delta)$ changes abruptly, which in turn affects the energy E_N^1. In contrast, the ground-state energy E_N^0 is a smooth function of c, and the solution Λ_N^0 has the same structure for all $c^2 > 0$. The structure of solutions $\Lambda_N^1(c < \sqrt{\Delta}, \Delta)$ and $\Lambda_N^1(c > \sqrt{\Delta}, \Delta)$ are shown in Fig. 7. Note that λ_1 never actually reaches zero, and λ_2 never reaches exactly $-\frac{\Delta}{c}$. From Fig. 7 it can be seen that the structure of the solution $\Lambda_N^1(c,\Delta)$ changes dramatically once c^2 crosses Δ.

Using this knowledge of the structure of the states we can deduce the first excited-state energy for the case $c^2 > \Delta$. As we discuss above, this state and its excitations has essentially the same structure as the ground state as described in Sec. IV B except that it has a overall energy shift of ΔN compared to the ground state. We can therefore use the same expression as

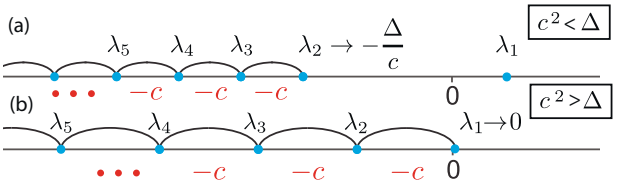

FIG. 7. Structure of the first excited-state solution $\Lambda_N^1(c,\Delta)$ of the Bethe equations (14) for (a) $c^2 < \Delta$ and (b) $c^2 > \Delta$.

Eq. (17), but shifted by the energy offset

$$E_N^1 \approx \Delta N - \frac{N+1}{c^2(N-1)+\Delta}, \tag{30}$$

which is valid for $c^2 > \Delta$. By substituting Eq. (30) into Eq. (12), this can equivalently be written

$$\mathcal{E}_N^1 \approx \frac{J^2(N+1)}{(U-V)(N-1)+2\epsilon} + \frac{U}{2}N(N-1) - \epsilon N, \tag{31}$$

which is valid for $U - V > 2\epsilon$.

3. *Error analysis*

In this section we compare the results which have been obtained by the application of our approximate method with the results which have been obtained numerically by exact diagonalization of the matrices (4) and (11), and also by numerical solution of the Bethe equations (14). We also would like to notice that the numerical results obtained by exact diagonalization and by application of the formulas (14) and (13) coincide completely, which ensures that the formalism described in Sec. III is correct.

In Fig. 4 the relative errors are shown for Eqs. (26) and (27), which are valid in the regime $c^2 < \Delta$. As expected, Eq. (26) fails for large c, where it is beyond its region of validity. From Fig. 5 it is evident that the precision of the formulas (26) and (27) increases with N. For Eq. (26) we find that $\alpha \simeq 2.0$, and $\alpha \simeq 2.9$ for Eq. (27). The divergent behavior of Eq. (26) is caused by E_N^1 crossing zero, which causes the relative error to take large values. This is really an artifact of our choice of the zero point of the energy, and is not related to any physical effects occurring in the system.

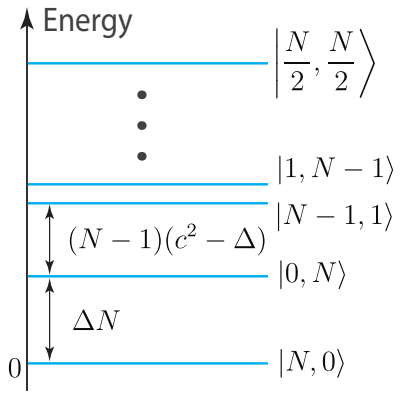

FIG. 8. Spectrum of the zero-tunneling Hamiltonian (28) for $c^2 > \Delta$.

Figure 6 shows Eq. (30), which is valid in the regime $c^2 > \Delta$. The energy of the first excited state agrees well with the exact expression for the parameters chosen. The relative errors of Eqs. (30) and (31) are shown in Fig. 4. The accuracy increase again follows a power law as seen in Fig. 5. We obtain $\alpha \simeq 3.0$ for Eq. (30) and $\alpha \simeq 4.0$ for Eq. (31).

V. EXPECTATION VALUES

We have seen that the equidistant approximation (16) works extremely well for estimating energies, because it perfectly predicts the first few roots which make the biggest contribution to Eq. (13). In this section we see whether other physical quantities can be estimated using the same approximation. To evaluate expectation values we express the eigenvectors of Hamiltonians (1) and (8) via solutions of Bethe equations, and discuss possible generalizations of the equidistant approximation. The expansion of Bethe vectors [30,31] into Fock space was performed in Ref. [49]. Since in the present paper we work mostly with the auxiliary Hamiltonian (8), it is slightly more convenient to use another representation of the Bethe vectors, which is given in Ref. [48], and give its expansion into a Fock space.

The Bethe state vectors for Hamiltonian (8) according to Ref. [48] are

$$|\Psi_N(\Lambda)\rangle = \sum_{m=0}^{N} e_m (b^\dagger)^m \mathbf{X}^{N-m} |0\rangle_a \otimes |0\rangle_b,$$

$$\langle\Psi_N(\Lambda)| = \langle 0|_b \otimes \langle 0|_a \sum_{m=0}^{N} e_m a^m \mathbf{Y}^{N-m}, \tag{32}$$

where e_m is the elementary symmetric function [61]:

$$e_m = \sum_{i_1<i_2<\cdots<i_m} \lambda_{i_1}\lambda_{i_2}\cdots\lambda_{i_m}, \tag{33}$$

and operators $\mathbf{X},\mathbf{Y}$ are defined as

$$\mathbf{X} = c^{-1}\Delta b^\dagger + c a^\dagger a b^\dagger + c^{-1} a^\dagger,$$
$$\mathbf{Y} = c^{-1} b + c a b^\dagger b. \tag{34}$$

Despite the fact that vectors (32) are not normalized and not Hermitian conjugates of each other, they form a complete orthogonal set, with which one can evaluate any observable [33]. Specifically, to evaluate the expectation value of an observable A one must calculate

$$\langle A\rangle = \frac{\langle\Psi_N(\Lambda)|\hat{A}|\Psi_N(\Lambda)\rangle}{\langle\Psi_N(\Lambda)|\Psi_N(\Lambda)\rangle}. \tag{35}$$

To evaluate Eq. (35), it is convenient to expand the states (32) into Fock space. Using standard commutation relations one may obtain the relation

$$(\alpha n_a + a^\dagger)^M |0\rangle = \sum_{k=0}^{M} D(M,k)\alpha^{M-k}(a^\dagger)^k |0\rangle, \tag{36}$$

where $D(M,k)$ are coefficients defined by the following recurrence relation:

$$D(M,k) = kD(M-1,k) + D(M-1,k-1) \tag{37}$$

with the conditions $D(1,1) = 1$ and $D(M,k) = 0$ if $k > M$. This coefficient possesses the obvious property: $D(M,1) = D(n,n) = 1$. The general expression for $D(M,k)$ is given by

$$D(M,k) = \sum_{n_1=0}^{M-k}\sum_{n_2=0}^{M-k-n_1}\sum_{n_3=0}^{M-k-n_1-n_2}\cdots \times \sum_{n_{k-1}=0}^{M-k-n_1-\cdots-n_{k-1}} k^{n_1}(k-1)^{n_2}\cdots 2^{n_{k-1}}. \tag{38}$$

By applying the binomial expansion for commuting operators in Eq. (34) and applying Eq. (36), we can expand the operators in Eq. (32) to yield the expressions

$$|\Psi_N(\{\lambda\})\rangle = \sum_{m=0}^{N}\sum_{l=0}^{N-m}\sum_{k=0}^{l}\sqrt{k!}\sqrt{(N-k)!}D(l,k) \times \binom{N-m}{l}\Gamma_{lmk}|k\rangle_a \otimes |N-k\rangle_a,$$

$$\langle\Psi_N(\{\lambda\})| = \sum_{m=0}^{N}\sum_{k=0}^{N-m}\langle N-k|_a \otimes \langle k|_b\sqrt{k!} \times \sqrt{(N-k)!}c^{-2k-m+N}D(N-m,k)e_m, \tag{39}$$

where the coefficient Γ_{lmk} is defined as

$$\Gamma_{lmk} = \Delta^{N-m-l}c^{-N+m+2l-2k}e_m. \tag{40}$$

To test the above formalism, we evaluated $\langle ab^\dagger\rangle$ for the ground state with different sets of parameters N,c, and Δ. We obtained results which deviated significantly from the exact result computed numerically, specifically for the parameters $N = 10$, $c = 1.0$, and $\Delta = 0.5$ where the obtained estimate differs by a factor of 10 from the exact value. We attribute this to a poor estimate of e_m using the equidistant approximation, which is not surprising. From Eq. (33) it can be noticed that the value of e_m depends on all the roots, and the largest contribution is given by the last few roots. In contrast to the energy in Eq. (13), the expression (33) is very sensitive to any deviation from the exact value for any of the roots. From Fig. 9 one can see that the last roots are predicted poorly from the equidistant approximation, which explains the poor performance for the expectation values. We would like to note, however, that Eq. (39) has been checked numerically and application of the exact solution of the Bethe equations (14) for the evaluation of e_m leads us to the correct result. While it appears that evaluating expectation values in the general case is rather difficult, there is

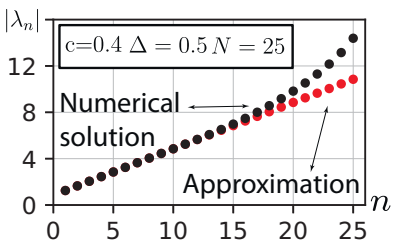

FIG. 9. Numerical and approximate solutions of the Bethe equations (14) corresponding to the ground state, for $c = 0.4$, $\Delta = 0.5$, and $N = 25$.

a possibility that evaluating certain types of correlations may still be possible using approximate methods that we discuss here. For example, energies are nothing but the expectation value of the Hamiltonian, and this can be evaluated efficiently. Thus similar quantities that are related to the Hamiltonian may be possible to calculate efficiently.

VI. SUMMARY AND CONCLUSIONS

In this paper we used the QIM formalism to obtain approximate analytical formulas for the ground-state and the first excited-state energies, for attractive interactions $U < V$ of the two-site Bose-Hubbard model. For the reader who is disinterested in the QIM formalism, the main results are Eq. (18) for the ground-state energy, Eq. (27) for the first excited state for $U - V < 2\epsilon$, and Eq. (31) for $U - V > 2\epsilon$. The obtained formulas work with remarkable precision for a wide range of parameters. Due to the nature of the QIM solutions, the expressions work well as long as the parameter $c^2 = (U - V)/J$ is not too small; for typical cases where $N > 10^3$, the accuracy is better than 1% for all formulas as long as $c^2 > 0.01$. The errors of the formulas tend to increase with N, with better than linear scaling seen for all cases.

Our formulas are based upon an equidistant approximation for the solution of the Bethe equations, which were obtained by analyzing the structure of the roots. Solving the Bethe equations has a comparable computational difficulty to solving the original Hamiltonian itself, which is the major drawback for practical use of the QIM formalism in the context of the Bose-Hubbard model. Our approximate solutions for the roots makes the practical use of the QIM solutions possible, yielding the relatively simple formulas for the energies. The high accuracy of the energies despite the approximate solution of the Bethe equations is due to the relative insensitivity of the energy formula (13) to roots with small magnitudes. Unfortunately, this is not true of evaluating expectation values, which is more sensitive to all the roots of a given state. This makes the equidistant approximation a poor choice in this case. An obvious extension of this work would be to find a similar approximate solution of the Bethe equations for the repulsive case $U > V$. This is equivalent to finding the solutions of the most excited states in Fig. 2. The qualitatively different structure of the roots has prevented us from obtaining a similar ansatz solution in this paper, but we do not see any fundamental reason why this would not be possible.

ACKNOWLEDGMENTS

This work is supported by the Shanghai Research Challenge Fund; New York University Global Seed Grants for Collaborative Research; National Natural Science Foundation of China (61571301); the Thousand Talents Program for Distinguished Young Scholars (D1210036A); the NSFC Research Fund for International Young Scientists (11650110425); NYU-ECNU Institute of Physics at NYU Shanghai; the Science and Technology Commission of Shanghai Municipality (17ZR1443600); and the China Science and Technology Exchange Center (NGA-16-001). I.E. and N.B. would like to thank the Russian Science Foundation (Grant No. 16-11-10218) for financial support.

[1] L. Pitaevskii and S. Stringari, *Bose-Einstein Condensation and Superfluidity*, Vol. 164 (Oxford University, Oxford, 2016).
[2] M. O. Scully and M. S. Zubairy, *Quantum Optics* (Cambridge University Press, New York, 1999).
[3] P. Y. Yu and M. Cardona, *Fundamentals of Semiconductors: Physics and Materials Properties* (Springer-Verlag, Berlin Heidelberg, 2010).
[4] M. E. Peskin, *An Introduction to Quantum Field Theory* (Westview, Boulder, CO, 1995).
[5] K. B. Davis, M.-O. Mewes, M. R. Andrews, N. J. van Druten, D. S. Durfee, D. M. Kurn, and W. Ketterle, Phys. Rev. Lett. **75**, 3969 (1995).
[6] M. H. Anderson, J. R. Ensher, M. R. Matthews, C. E. Wieman, E. A. Cornell *et al.*, Science **269**, 198 (1995).
[7] I. Bloch, Nat. Phys. **1**, 23 (2005).
[8] T. Byrnes, N. Y. Kim, and Y. Yamamoto, Nat. Phys. **10**, 803 (2014).
[9] I. Georgescu, S. Ashhab, and F. Nori, Rev. Mod. Phys. **86**, 153 (2014).
[10] R. Fazio and H. Van Der Zant, Phys. Rep. **355**, 235 (2001).
[11] J. Klaers, J. Schmitt, F. Vewinger, and M. Weitz, Nature **468**, 545 (2010).
[12] T. Nikuni, M. Oshikawa, A. Oosawa, and H. Tanaka, Phys. Rev. Lett. **84**, 5868 (2000).
[13] S. Demokritov, V. Demidov, O. Dzyapko, G. Melkov, A. Serga, B. Hillebrands, and A. Slavin, Nature **443**, 430 (2006).
[14] H. Tiecke, I. Shvarchuck, W. Von Klitzing, M. Kemmann, C. Buggle, and J. Walraven, J. Opt. B **5**, S119 (2002).
[15] C. Gross, J. Phys. B **45**, 103001 (2012).
[16] M. Albiez, R. Gati, J. Fölling, S. Hunsmann, M. Cristiani, and M. K. Oberthaler, Phys. Rev. Lett. **95**, 010402 (2005).
[17] T. Schumm, S. Hofferberth, L. Andersson, S. Wildermuth, S. Groth, I. Bar-Joseph, J. Schmiedmayer, and P. Krüger, Nat. Phys. **1**, 57 (2005).
[18] J. Estève, C. Gross, A. Weller, S. Giovanazzi, and M. Oberthaler, Nature **455**, 1216 (2008).
[19] C. Gross, T. Zibold, E. Nicklas, J. Estève, and M. Oberthaler, Nature **464**, 1165 (2010).
[20] M. F. Riedel, P. Böhi, Y. Li, T. W. Hänsch, A. Sinatra, and P. Treutlein, Nature **464**, 1170 (2010).
[21] Q. Y. He, M. D. Reid, T. G. Vaughan, C. Gross, M. Oberthaler, and P. D. Drummond, Phys. Rev. Lett. **106**, 120405 (2011).
[22] Q. Y. He, P. D. Drummond, M. K. Olsen, and M. D. Reid, Phys. Rev. A **86**, 023626 (2012).
[23] L. Pitaevskii and S. Stringari, Phys. Rev. Lett. **87**, 180402 (2001).
[24] K. Pawłowski, P. Ziń, K. Rzazewski, and M. Trippenbach, Phys. Rev. A **83**, 033606 (2011).
[25] D. Rubeni, J. Links, P. S. Isaac, and A. Foerster, Phys. Rev. A **95**, 043607 (2017).
[26] T. Byrnes, K. Wen, and Y. Yamamoto, Phys. Rev. A **85**, 040306 (2012).

[27] T. Byrnes, D. Rosseau, M. Khosla, A. Pyrkov, A. Thomasen, T. Mukai, S. Koyama, A. Abdelrahman, and E. Ilo-Okeke, Opt. Commun. **337**, 102 (2015).
[28] G. J. Milburn, J. Corney, E. M. Wright, and D. F. Walls, Phys. Rev. A **55**, 4318 (1997).
[29] T. Pudlik, H. Hennig, D. Witthaut, and D. K. Campbell, Phys. Rev. A **90**, 053610 (2014).
[30] V. Enol'skii, V. Kuznetsov, and M. Salerno, Phys. Nonlinear Phenom. **68**, 138 (1993).
[31] J. Links and K. E. Hibberd, SIGMA **2**, 095 (2006).
[32] L. Faddeev, in *40 Years in Mathematical Physics* (World Scientific, Singapore, 1995), pp. 187–235.
[33] V. E. Korepin, N. M. Bogoliubov, and A. G. Izergin, *Quantum Inverse Scattering Method and Correlation Functions*, Vol. 3 (Cambridge University, Cambridge, England, 1997).
[34] E. K. Sklyanin, L. A. Takhtadzhyan, and L. D. Faddeev, Theor. Math. Phys. **40**, 688 (1979).
[35] P. P. Kulish and E. K. Sklyanin, in *Integrable Quantum Field Theories* (Springer, New York, 1982), pp. 61–119.
[36] V. E. Korepin, Commun. Math. Phys. **86**, 391 (1982).
[37] L. D. Faddeev, *Fifty Years of Mathematical Physics: Selected Works of Ludwig Faddeev* (World Scientific, Singapore, 2016), pp. 370–439.
[38] J.-M. Maillet, *Quantum Spaces*, edited by B. Duplantier (Birkhäuser, Basel, 2007), pp. 161–201.
[39] F. Levkovich-Maslyuk, J. Phys. A **49**, 323004 (2016).
[40] N. Kitanine, J. Maillet, and V. Terras, Nucl. Phys. B **554**, 647 (1999).
[41] G. Kato, M. Shiroishi, M. Takahashi, and K. Sakai, J. Phys. A **36**, L337 (2003).
[42] M. Bortz and F. Göhmann, Eur. Phys. J. B **46**, 399 (2005).
[43] E. H. Lieb and W. Liniger, Phys. Rev. **130**, 1605 (1963).
[44] M. Knap, C. J. M. Mathy, M. Ganahl, M. B. Zvonarev, and E. Demler, Phys. Rev. Lett. **112**, 015302 (2014).
[45] N. M. Bogoliubov and P. P. Kulish, Zap. Nauchn. Semin. POMI **398**, 26 (2012).
[46] G. Arutyunov, S. Frolov, and M. Staudacher, J. High Energy Phys. 10 (2004) 016.
[47] T. Thiery and P. Le Doussal, J. Phys. A **50**, 045001 (2016).
[48] N. Bogoliubov, J. Math. Sci. **213**, 662 (2016).
[49] G. Santos, C. Ahn, A. Foerster, and I. Roditi, Phys. Lett. B **746**, 186 (2015).
[50] F. Dominguez, C. Esebbag, and J. Dukelsky, J. Phys. A **39**, 11349 (2006).
[51] R. Vieira and A. Lima-Santos, Phys. Lett. A **379**, 2150 (2015).
[52] R. Hagemans and J.-S. Caux, J. Phys. A **40**, 14605 (2007).
[53] P. Dorey, C. Dunning, and R. Tateo, J. Phys. A **40**, R205 (2007).
[54] F. Dalfovo, S. Giorgini, L. P. Pitaevskii, and S. Stringari, Rev. Mod. Phys. **71**, 463 (1999).
[55] C. Chin, R. Grimm, P. Julienne, and E. Tiesinga, Rev. Mod. Phys. **82**, 1225 (2010).
[56] Y.-J. Lin, K. Jiménez-García, and I. Spielman, Nature **471**, 83 (2011).
[57] A. J. Olson, D. L. Whitenack, and Y. P. Chen, Phys. Rev. A **88**, 043609 (2013).
[58] T.-L. Ho and V. B. Shenoy, Phys. Rev. Lett. **77**, 3276 (1996).
[59] C. C. Bradley, C. A. Sackett, and R. G. Hulet, Phys. Rev. Lett. **78**, 985 (1997).
[60] A. A. Vladimirov, Theor. Math. Phys. **66**, 102 (1986).
[61] I. G. Macdonald, *Symmetric Functions and Hall Polynomials* (Oxford University, Oxford, 1998).